Investigation of structural, dynamical, electronic and magnetic properties of MX_2(M = Mo, X = Se, Te) materials

Kamal Khanal*, Arpan Pokharel*, Tejendra Neupane*, Sukrit Kumar Yadav*, Nabin Aryal*, Om Shree Rijal* and Hari Krishna Neupane*

***Amrit Campus, Institute of Science and Technology, Tribhuvan University, Kathmandu Nepal.**

Abstract: Two-dimensional (2D) transition metal dichalcogenides (TMDCs) materials have potential applications in the field of device applications. In the present work, we explored the structural, dynamical, electronic, and magnetic properties of $MoSe_2$ and $MoTe_2$ TMDCs materials by using density functional theory (DFT) method. For the investigation of material's structural and dynamical stability, we have estimated their ground state energies, bond length of atoms presented in the structures, and phonon dispersion curves respectively. They are found to be structurally and dynamically stable materials. Furthermore, we have studied the electronic and magnetic properties of $MoSe_2$ and $MoTe_2$ materials. Electronic properties are investigated by the analysis of their band structure, and density of states (DOS) plots. Both the materials are found to be small band gap p-type semiconductor. For the investigation of material's magnetic properties, we have interpretated the DOS and partial density of states (PDOS) plots. In both plots, up-and down-spin states are symmetrically distributed around the Fermi energy level. They reveal that $MoSe_2$ and $MoTe_2$ have non-magnetic properties. Based on the multi-properties investigation of $MoSe_2$ and $MoTe_2$, they can be used in a variety of device applications, including optoelectronic, semiconducting, energy storage, and sensing devices.

Keywords: Dynamical; Electronic; Magnetic; Monolayer; Semiconductor.

Introduction

Discovery of graphene in 2004, raised a lot of interest to the study of two-dimensional (2D) layered materials due to their small size and better performance than their 3D counterparts[1]. Other than graphene, transition metal dichalcogenides (TMDCs) materials have potential applications in the field of nanoelectronics[2, 3]. The general formula of TMDCs materials is MX_2 where, M is transition metal and X is chalcogen[2]. Molybdenum di-Sulphide (MoS_2) is a TMDCs material which has lot of applications in the field of nanoelectronics devices because of it structural and electronic properties[3]. The Molybdenum and Tungsten based TMDCs materials have huge interest in the device applications due to their semi-conducting behavior, having broad band gaps spanning from visible to near-infrared region[4]. Moreover, Molybdenum di-Selenide ($MoSe_2$) and Molybdenum di-Telluride ($MoTe_2$) are the family of TMDCs materials, which are formed having one part Molybdenum and two parts of Selenium and Tellurium atoms in $MoSe_2$ and $MoTe_2$ respectively[5]. These materials have higher electrical conductivity and electron mobility as compared to MoS_2. These properties of materials are important for high-performance electronic devices[6]. Similarly, $MoSe_2$ and $MoTe_2$ have strong photoluminescence (PL), which is important for the optical properties of materials[2, 7]. Due to strong PL properties of $MoSe_2$ and $MoTe_2$, they have high

Author for correspondence: Hari Krishna Neupane, Amrit Campus, Institute of Science and Technology, Tribhuvan University, Kathmandu Nepal.
Email: hari.neupane@ac.tu.edu.np; https://orcid.org/0000-0001-8547-1183
Received: 17 Mar, 2025; Received in revised form: 3 Apr, 2025; Accepted: 16 Apr, 2025.
Doi: https://doi.org/10.3126/sw.v18i18.78446

light absorption and emission capacity.

It makes them appropriate for the application in photodetectors, solar cells etc. [7]. The electronic properties of material are important which are tuned by the factors like strain, electric fields, and chemical doping [8]. $MoSe_2$ can is used for energy storing devices such as lithium-ion batteries and supercapacitors due to their layered structure and large surface area [9]. The heterostructure of TMDCs materials are promising materials for solar energy conversion because heterostructure can improve charge separation and lower recombination losses [10]. They can be used specially in nanotechnology and biomedical field [11]. $MoSe_2$ and $MoTe_2$ have great applications in the field of nanoelectronics devices due to their flexibility and stability properties [10, 11, 12]. So, the rigorous investigation of $MoSe_2$ and $MoTe_2$ TMDCs materials become hot topic in the field condensed matter physics and material science in the present days [12, 13]. For this reason, we have reviewed the literature relating to the properties of 2D and TMDCs materials and found that doped or vacancy defected $MoSe_2$ and $MoTe_2$ have magnetic properties, and hence they can be used in the fields of spintronics applications [13, 14, 15, 16]. On the other hand, we have reviewed a lot of literatures regarding to TMDCs materials. Literature suggests that detailed study of structural, electronic, magnetic and dynamical properties of (3×3) supercell of $MoSe_2$ and $MoTe_2$ monolayer have not been done properly. These are the research questions of the present study. Hence, our motivation goes to study in details about the structural, electronic, dynamical, and magnetic properties of (3×3) supercell of $MoSe_2$ and $MoTe_2$ monolayer computationally under density functional theory (DFT) method through quantum ESPRESSO (QE) as a computational tool.

Computational details

Spin-polarized density functional theory (DFT) approach has been carried out with the use of plane wave basis set by using ultrasoft pseudopotentials (USPPs) under computational tool quantum ESPRESSO (QE) [17, 18, 19]. To study exchange-correlation energy (EX-C), Perdew-Burke- Ernzerhof (PBE) functional has been used from generalized gradient approximation (GGA) [20]. XmGrace and XCrySDen are used as a software package for the graph plotting and structure visualization [21, 22]. First of all, we have prepared a unit cell of $MoSe_2$ and $MoTe_2$ monolayers, then optimized these structures by the estimation of their kinetic energy cutoff, k-points and lattice parameters values through self-consistency functional (scf) calculations. The relaxed structure is secured after the optimization of k-points, kinetic energy cutoff, and lattice parameters. The Brillouin zone (BZ) has been sampled by using Monkhorst-Pack (MP) [23] with a (12×12×1) k-point grid. Similarly, the kinetic energy cutoffs for the plane wave basis set are taken 471 eV (34.61 Rydberg) and 690 eV (50.71 Rydberg) for $MoSe_2$ and $MoTe_2$ respectively. They are estimated by the optimization of parameters. The optimized value of lattice parameter of $MoSe_2$ and $MoTe_2$ are found to be 5.83 Å and 5.90 Å values respectively. We extended that optimized and relax unit cell structures of $MoSe_2$ and $MoTe_2$ monolayers by three times along x-axis, three times along y-axis to create desired (3×3) supercell structure. Then, relax calculations are done of these supercell structures through scf calculations. Further calculations of optimized and relax supercell structures of $MoSe_2$ and $MoTe_2$ are performed. Structural properties of considered materials are studied by the calculations of their ground state energies and bond length of atoms present in the materials.

The phonon dispersion curves are used to check the material's dynamical stability (properties). These phonon calculations are done by using density functional perturbation theory (DFPT) techniques [24]. Additionally, we have investigated the electronic and magnetic properties of considered supercell structures by the interpretation of their band structure & density of states (DOS), and DOS & partial density of states (PDOS) calculations. In DOS and PDOS calculations, we have used denser mesh of (22×22×1) k-point grid because denser grid makes smooth DOS/PDOS states in DOS & PDOS plots.

Results and Discussion

In this section, we present an interpretation of major findings of $MoSe_2$ and $MoTe_2$ materials.

a. Structural properties

The structural properties of $MoSe_2$ and $MoTe_2$ monolayer materials have been studied by calculating their ground state energy, and bond length between the nearest atoms present in structures. The optimized and relax structures of $MoSe_2$ and $MoTe_2$ supercell monolayers are shown in figures-1(a - d) respectively.

We have estimated the ground state energy of $MoSe_2$ and $MoTe_2$ monolayer supercell structures are found to be -244.20 eV and -248.10 eV respectively. They are similar values of others TMDCs materials [25, 26]. These minimum ground states energy of both materials reflects that they are stable materials. It is well known that any materials are said to be structurally stable having their minimum ground state energy. Hence, these (3×3) supercell structures of $MoSe_2$ and $MoTe_2$ are stable 2D monolayer material.

Moreover, we have estimated the bond length in between Mo-Mo, Mo-Se, Se-Se in $MoSe_2$ and Mo-Mo, Mo-Te, Te-Te atoms in $MoTe_2$ materials respectively. They are found to be 3.31 Å, 2.54 Å, & 3.31 Å in $MoSe_2$, and 3.31 Å, 2.56 Å, & 3.35 Å in $MoTe_2$. These estimated values of interatomic bonding of atoms in the $MoSe_2$ and $MoTe_2$ have nearly equal values of reported works of TMDCs materials [8, 27, 28]. The estimated and reported interatomic distance of present atoms in the structures are given in Table-1.

Table 1: The estimated and reported values of interatomic distances between Mo-Se, Mo-Te, Mo-Mo, Se-Se, and Te-Te atoms in $MoSe_2$ and $MoTe_2$ supercell structures are given in tabular form.

Materials	Estimated	Reported	Estimated	Reported	Estimated	Reported
$MoSe_2$	Mo-Se = 2.54 Å	2.53 Å [8]	Mo-Mo=3.31Å	3.30 Å [8]	Se-Se = 3.31 Å	3.34 [8]
$MoTe_2$	Mo-Te = 2.56 Å	2.73 Å [28]	Mo-Mo=3.31Å	3.30 Å [8]	Te-Te = 3.35 Å	3.51 Å [27]

From the above explanation, it is confirmed that our considered TMDCs materials are structurally stable.

b. Dynamical properties

A phonon dispersion curve describes the relationship between the frequency of phonons and their wave vector, providing insights into the vibrational properties of the lattice. To examine the dynamical stability of material, phonon dispersion curves have been studied. In the present work, we have analyzed the phonon dispersion curves to test the dynamic stability of $MoSe_2$ and $MoTe_2$ materials. Phonon calculations are done by using GGA with PBE functional. Figures-2(a & b) respectively, represent the phonon dispersion plots of $MoSe_2$ and $MoTe_2$ materials

In figure-2, it is seen that there are no negative values of phonon frequency in the Brillouin zone. It indicates that $MoSe_2$ and $MoTe_2$ monolayers are dynamically stable because materials are said to be dynamical stable due to their positive values of phonon frequency [29]. There is total nine vibration modes for both systems. Among them, three are acoustic modes, and six are optical modes, which are shown in figures-2(a & b). In figures, lower branch is known as acoustic branches, represented by red lines whereas upper branch named as optical branches, which are represented by green lines. From the phonon dispersion plots, we can see that acoustic waves have zero frequency at Γ point, but frequency of optical branch has minimum value of 4.90 cm^{-1} and 4.01 cm^{-1} at Γ position of $MoSe_2$ and $MoTe_2$ materials respectively. Moreover, at symmetric points M, K, A, L, & H have maximum frequency for acoustic waves, which are approximately equal (4.73, 4.57, 4.71, 4.38 & 4.76) cm^{-1} respectively of both materials. Similarly, looking the minimum optical frequencies at M, K, A, L, & H, it is found to be (5.35, 5.71, 5.35, 5.65 & 5.34) cm^{-1} respectively, of $MoSe_2$, and (4.12, 4.31, 4.05, 4.15 & 4.06) cm^{-1} respectively, of $MoTe_2$ materials. The phonon frequencies at each symmetric point show that optical phonons oscillate more rapidly than acoustic phonons, which matches the theoreticalprediction [30]. The phonon band gap of $MoSe_2$ has found to be (0.92, 1.14, 0.64, 1.27, 0.38) cm^{-1} respectively at M, K, A, L & H symmetric points, and $MoTe_2$ has found to be (0.61, 0.26, 0.66, 0.23, & 0.70) cm^{-1} respectively at M, K, A, L & H symmetric points. These values are existed between the lower point of optical branches and upper points of acoustical branches at

symmetric points. The zero value of phonon frequency at Γ point of the acoustic modes give another evidence of dynamical stability of $MoSe_2$ and $MoTe_2$ monolayers materials. Hence, the considered materials are found to be dynamically stable. From above calculations, it is found that the minimum optical band gap of $MoSe_2$ has 0.23 cm^{-1} at L symmetric point respectively.

c. Electronic properties

To understand the distribution of electron and electronic energy in material, electronic properties play a vital role.

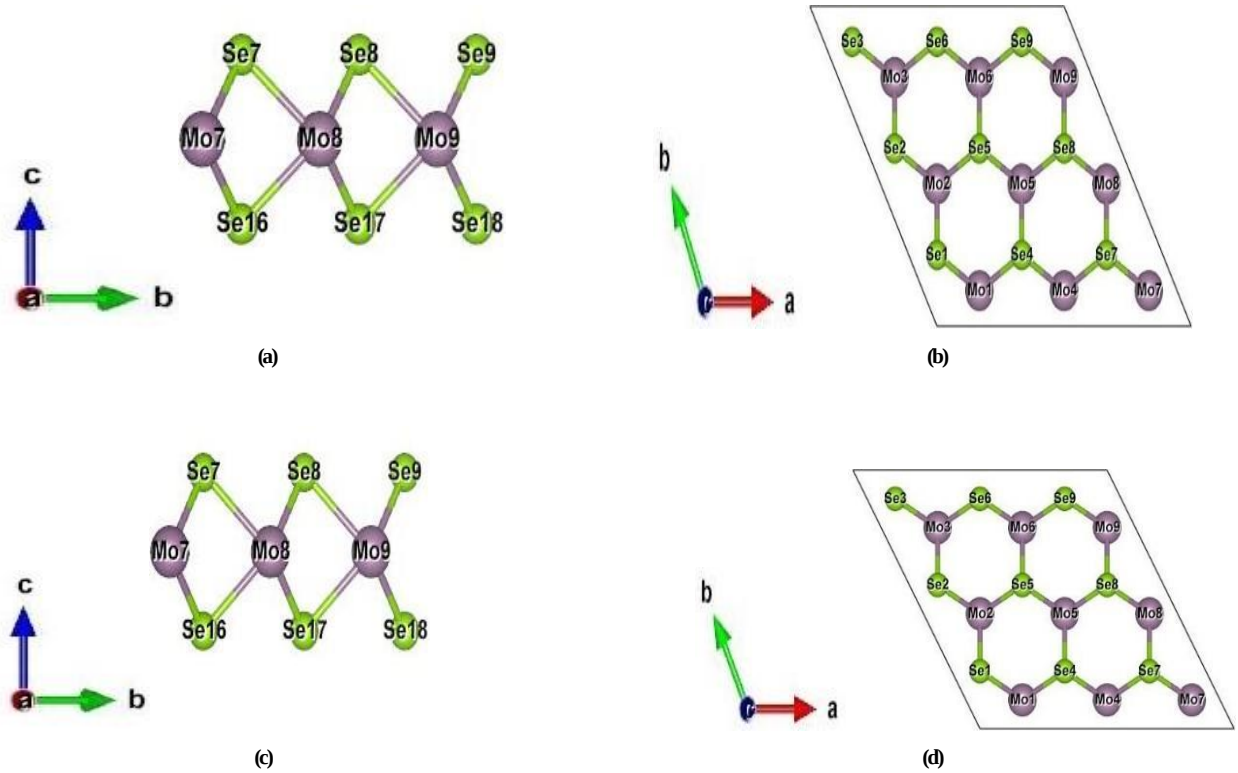

Figure 1: (Colour online) Supercell structure of $MoSe_2$ and $MoTe_2$ TMDCs materials: (a) front view of $MoSe_2$ supercell structure, (b) top view of $MoSe_2$ supercell structure, (c) front view of $MoTe_2$ suprecell structure, and (d) top view of $MoTe_2$ supercell structure.

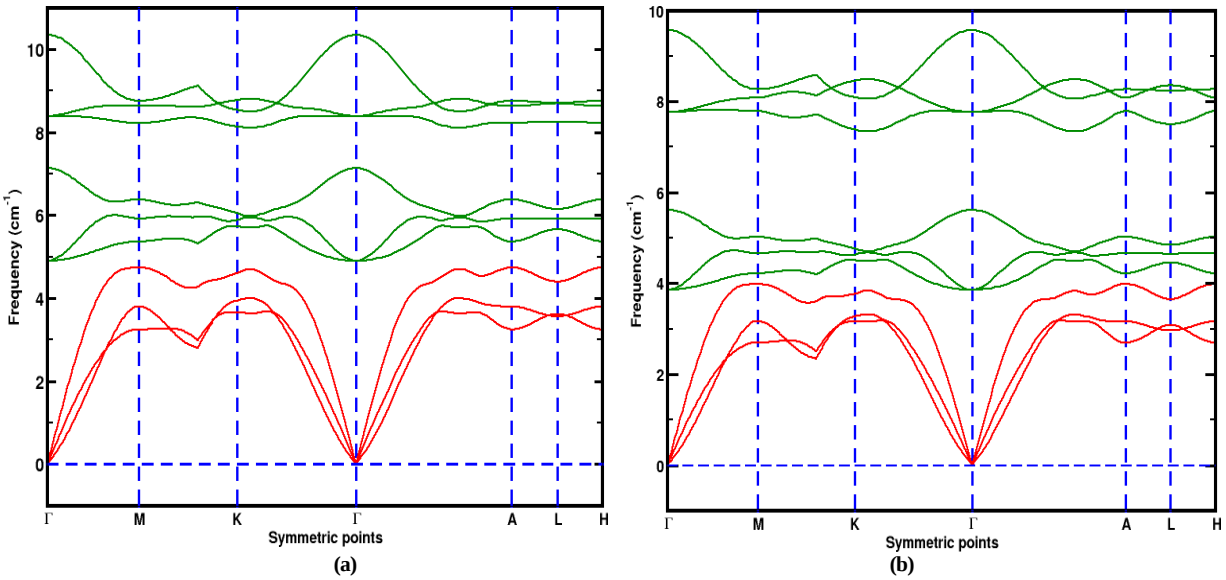

Figure 2: (Colour online) Phonon dispersion curve of; (a) $MoSe_2$ material, and (b) $MoTe_2$ material. In both plots, high symmetric points (k-vector) are taken along the x-axis, and rate of vibration in terms of wave number (frequency) are taken along the y-axis. The vertical dot lines touch highly symmetric points in the Brillion zone.

To study the electronic properties, the band structure and density of states (DoS) of $MoSe_2$ and $MoTe_2$ monolayer have been discussed. Figures-3(a & b) respectively illustrated the band structure plots of $MoSe_2$ and $MoTe_2$ materials, where highly symmetric points are plotted along the x-axis and corresponding energy values are taken along the y-axis. The horizontal dotted line is called Fermi energy level, which separates the electronic bands. The region below the Fermi level is called valence band, while the region above the Fermi level is called conduction band.

In figure-3(a), it is found that band gap energy at gama (Γ) point of $MoSe_2$ material has value 1.57 eV. It is obtained by the energy form conduction band minimum (CBM) to Fermi level and valence band maximum (VBM) to Fermi level. The value of CBM to Fermi energy level is found to be 1.42 eV, and VBM to Fermi energy level is found to be 0.15 eV. Similarly, the bandgap energy of $MoTe_2$ material is found to be 1.52 eV. This value is obtained by summing the value of CBM to Fermi level of value 1.38 eV, and VBM to Fermi level of value 0.14 eV. The CBM and VBM in both materials are tracked down at Γ- point in the center of Brillouin zone. It is indicating that nature of band gap is direct. It is also seen that, there are more bands in the valance band region than the conduction band region, which reveals that both the materials have p-type semiconducting properties. The band gap energy values of $MoSe_2$ and $MoTe_2$ materials are found to be 1.57 eV and 1.52 eV respectively, they are closely agreeing with the reported value (1.50 eV) of TMDCs materials [30, 31, 32].

The density of states (DOS) plots of $MoSe_2$ and $MoTe_2$ materials are shown in figures-4(a & b) respectively, where horizontal dotted line separated the up-spin and down-spin states, while vertical dotted line represents the Fermi energy level. The DOS of spin states are plotted along the y- axis and their corresponding energy values are taken along the x- axis.

DOS plot is used to study the electronic properties as well as magnetic properties of material. It tells that how many electronic states are available at each energy level. At the Fermi energy level, Mo atom has dominant contribution than of Se atom in $MoSe_2$ material. Likewise, in $MoTe_2$ material, Mo atoms in material have leading contribution than Te atoms. It means, up-and down- spin states of Mo atoms have higher peaks than of others atoms, which reflects that there will be a greater number of unoccupied orbitals of atoms. We have estimated the band gap energy of both materials in materials in DOS plots. It is found that band gap energy of $MoSe_2$ has value 1.52 eV, and band gap energy value of $MoTe_2$ has value 1.50 eV. These both values are approximate band gap energy values obtained from the band structure plots of $MoSe_2$ and $MoTe_2$ materials. Thus, the DOS calculations also confirmed that considered materials are direct band gap p-type semiconductors. The estimated band gap energies of both materials are given in Table-2.

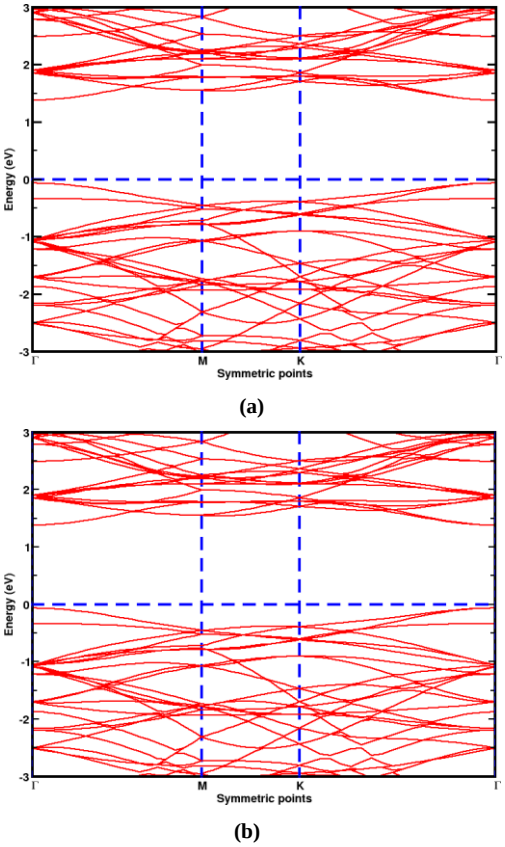

Figure 3: (Color online) band structure plots of: (a) $MoSe_2$ material, and (b) $MoTe_2$ material. Horizontal dash line at zero represent Fermi level and vertical dash line represent high symmetric points.

d. Magnetic properties

To determine a material's magnetic characteristics, density of states (DOS) and partial density of states (PDOS) analyses can be performed. DOS plot shows how many

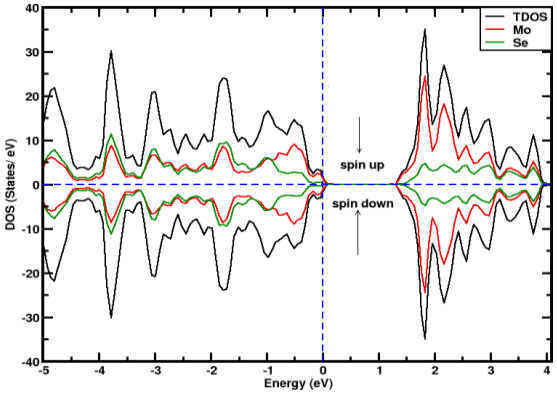

(a)

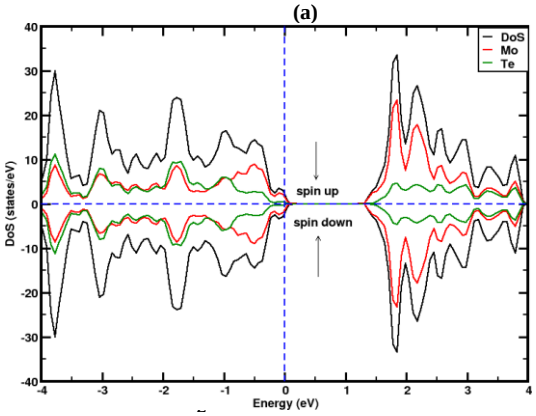

(b)

Figure 4: (Color online) Density of states (DOS) plot of $MoSe_2$ and $MoTe_2$ of materials; (a) DOS of $MoSe_2$ material, (b) DOS of $MoTe_2$ material.

Table 2: Band gap energy of $MoSe_2$ and $MoTe_2$ materials, which are estimated from the analysis of materials band structure and DOS plots.

Materials	From band structure		From DOS plots	
	Estimated values	Reported values	Estimated values	Reported values
$MoSe_2$	1.57 eV	1.50 eV [31, 32]	1.52 eV	1.50 eV [31, 32]
$MoTe_2$	1.52 eV	1.50 eV [31, 32]	1.50 eV	1.50 eV [31, 32]

electronic states are available within a material at each energy level. Similarly, PDOS plot describes which spin states in the orbital of atoms contribute the magnetic moment in the system[33]. If the up-and down-spin states of electrons in the orbitals of atoms are symmetrically distributed around the Fermi energy level, then the materials have non-magnetic properties. But, the asymmetrically distributed spin states of electrons in the orbitals of atoms indicate that materials have magnetic properties The PDOS plots of $MoSe_2$ and $MoTe_2$ materials are illustrated in figures-5(a & b) respectively. In figures, it is seen that PDOS states are taken along the y-axis, and their corresponding energies are taken along the x-axis. The horizontal dash line in both plots distinguished the distributed up-and down- spin states, while vertical dash line indicates the Fermi energy level, which separates the valence band and the conduction band. The left-hand side region from the dotted line is called the valence band and right-hand side region for the dotted line is called the conduction band.

Based on the DOS plots of $MoSe_2$ and $MoTe_2$ materials are shown in figures-4(a & b), it is seen that up-and down-spin states of total DOS are symmetrically distributed around the Fermi energy level. Hence, they are non-magnetic materials. The details analysis of magnetic properties in $MoSe_2$ and $MoTe_2$ materials are studied on the basis of their PDOS plots, which are illustrated in figures-5(a & b) respectively. Electronic configuration of Mo, Se, & Te atoms in $MoSe_2$ and $MoTe_2$ materials are [Kr] $4d^5\ 5s^1$, [Ar] $3d^{10}\ 4s^2\ 4p^4$, and [Kr] $4d^{10}\ 5s^2\ 5p^4$, respectively. The valance electron of the Mo atom exists in 4d and 5s orbitals, Se atom contains 4p orbital and Te atom has 5p orbital. In figure-5(a), it is seen that electronic structure of $MoSe_2$ monolayer is dominated by the hybridization between 4d orbital of Mo, $4d_{xy}$, $4d_x^2$, and $4d_z^2$ have highest contribution of magnetic moment near the Fermi energy level. Further, we have observed the PDOS of Se atom, it is found that $4p_y$, $4p_x$ and $4p_z$ sub-orbitals have greater contribution of magnetic moment than other sub-orbitals near the Fermi region. From the analysis of PDOS plot of $MoSe_2$, it is revealed that up-and down-spin states in the individual orbitals of Mo and Se atoms are symmetrically distributed around the Fermi energy level. The total magnetic moment given by all up-spin states have equal to total magnetic moment given by all down-spin states. The resultant value of magnetic moment is zero (0 μB/cell). Hence, $MoSe_2$ has non-magnetic properties. Similarly, figure-5(b) illustrates the PDOS plot $MoTe_2$. In this graph, it is seen that the Mo has similar contributions as to that of $MoSe_2$. From the PDOS of Te atoms, it is

found that 5p-orbital has greater contributions for the production of magnetic moment than other orbitals in the material. In details, 5py, 5px and 5pz sub-orbitals of Te atoms have dominant contribution for the production of magnetic moment.

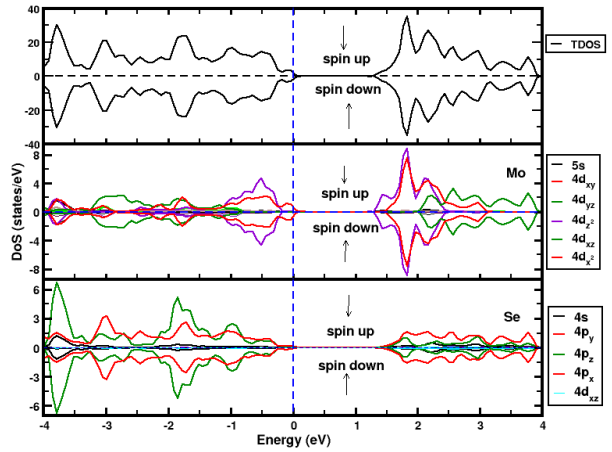

(a)

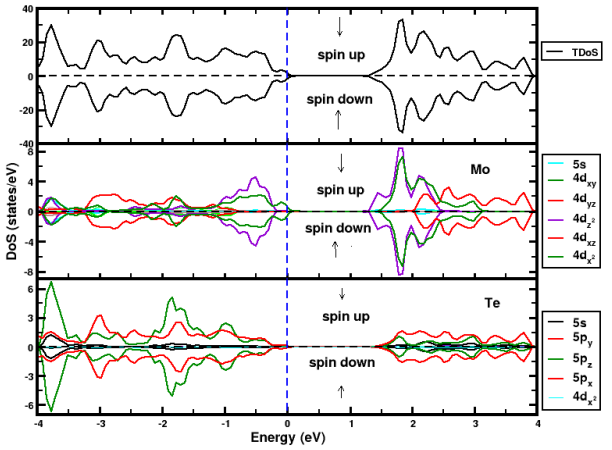

(b)

Figure 5: (Color online) Partial density of states (PDOS) plot of $MoSe_2$ and $MoTe_2$ of materials: (a) PDOS of $MoSe_2$ material, (b) PDOS of $MoTe_2$ material. In both plots, vertical dotted line represents the Fermi energy level which separated the electronic bands.

Similar like $MoSe_2$ material, it is found that up-and down-spin states of individual orbitals of Mo and Te atoms of $MoTe_2$ material are symmetrically distributed around the fermi energy level. It means, total magnetic moment given by up-spin are cancelled out by the magnetic moment given by total down-spin states, and hence resultant magnetic moment in the system is zero (0 μB/cell). Thus, $MoTe_2$ has non-magnetic properties. Therefore, from the analysis of DOS and PDOS plots of $MoSe_2$ and $MoTe_2$ materials, it is confirmed that both materials have non-magnetic nature. The detail calculations of magnetic moment of both materials are given in Table-3.

Table 3: Magnetic moment (μ) contributed by 5s, $4d_{xy}$, $4d_{yz}$, $4d_{xz}$, $4d_z^2$, $4d_x^2$ orbitals of Mo atoms, 4s, $4p_y$, $4p_z$, $4p_x$, $4d_{xz}$ orbitals of Se atoms, and 5s, $5p_y$, $5p_z$, $5p_x$, $4d_x^2$ orbitals of Te atoms presented in $MoSe_2$ and $MoTe_2$ materials.

Orbitals / Materials	$MoSe_2$		$MoTe_2$	
	Up-spin	Down-spin	Up-spin	Down-spin
μ of 5s_Mo atom (μ_B/cell)	0.01	-0.01	0.00	-0.00
μ of $4d_{xy}$_Mo atom (μ_B/cell)	8.00	-8.00	8.01	-8.01
μ of $4d_{yz}$_Mo atom (μ_B/cell)	4.00	-4.00	3.90	-3.90
μ of $4d_{xz}$_Mo atom (μ_B/cell)	4.01	-4.01	3.90	-3.90
μ of $4d_z^2$_Mo atom (μ_B/cell)	8.25	-8.25	8.20	-8.20
μ of $4d_{x^2}$_Mo atom (μ_B/cell)	8.00	-8.00	8.01	-8.01
μ of 4s_Se atom (μ_B/cell)	0.00	-0.00	-	-
μ of $4p_y$_Se atom (μ_B/cell)	3.00	-3.00	-	-
μ of $4p_z$_Se atom (μ_B/cell)	7.00	-7.00	-	-
μ of $4p_x$_Se atom (μ_B/cell)	3.00	-3.00	-	-
μ of $4d_{xz}$_Se atom (μ_B/cell)	0.02	-0.02	-	-
μ of 5s_Te atom (μ_B/cell)	-	-	0.00	-0.00
μ of $5p_y$_Te atom (μ_B/cell)	-	-	3.00	-3.00
μ of $5p_z$_Te atom (μ_B/cell)	-	-	7.20	-7.20
μ of $5p_x$_Te atom (μ_B/cell)	-	-	3.00	-3.00
μ of $4d_{x^2}$_Te atom (μ_B/cell)	-	-	0.02	-0.02
Total magnetic moment (μ)	45.29	-45.29	45.24	-45.24
Net magnetic moment (μ)	0.00 μ_B/cell		0.00 μ_B/cell	

Conclusions

In summary, we have explored the structural, dynamical, electronic and magnetic properties of $MoSe_2$ and $MoTe_2$ materials by using DFT method. The computational tool quantum ESPRESSO is used to perform the computations using GGA with PBE functional. Firstly, we have estimated the bond length between the nearest atoms in structures, and ground states energies of considered materials. These values are closely agreed with the reported value of others stable TMDCs materials. Based on the estimated values of materials, they are found to be structurally stable. Moreover, we have also examined the dynamical stability of considered materials through the calculations of phonon dispersion curves. It is found that phonon frequencies of $MoSe_2$ and $MoTe_2$ materials have

positive values at each symmetric point. Hence, it is also confirmed that studied materials are dynamically stable. Furthermore, the electronic and magnetic properties of $MoSe_2$ and $MoTe_2$ materials are investigated by the interpretations of material's band structure and density of states (DOS) and partial density of states (PDOS). Both $MoSe_2$ and $MoTe_2$ materials have small band gap energies of values 1.57 eV and 1.52 eV respectively. Also, from the DOS plots, the band gap energy of $MoSe_2$ and $MoTe_2$ are found to be 1.52 eV and 1.50 eV respectively. From the analysis of both band and DOS calculations, it is concluded that $MoSe_2$ and $MoTe_2$ are small band gap semiconducting materials. The magnetic properties of considered materials are predicted by the analysis of their DOS and PDOS plots. In both plots, up-and down-spin states are symmetrically distributed around the Fermi energy level. The $4d_x^2$, $4d_z^2$ sub-orbitals of Mo atoms, $4p_y$, $4p_x$, & $4p_z$ sub-orbitals of Se atoms, and $5p_y$, $5p_x$, & $5p_z$ sub-orbitals of Te atoms have dominant contribution for the production of magnetic moment, but the total magnetic moment given by up-spin and down-spin are cancelled out. It reflects that $MoSe_2$ and $MoTe_2$ have non- magnetic properties. From the comprehensive study of above-mentioned properties of $MoSe_2$ and $MoTe_2$, they can be used in optoelectronic, semiconducting, energy storage, and sensing devices.

Acknowledgement

The authors would like to acknowledge the condensed matter research lab CDP TU, TWAS research funds RG 20-316, network project NT-14 of ICTP/OE for the computing capacity, and Prof. NP Adhikari for his excellent input on the manuscript.

Author Contributions

KK, AP, TN, SKY, NA and OSR generated the data and wrote the manuscript using formal data analysis. HKN came up with the idea, managed the project, analyzed the information, and revised and assessed the text.

References

[1] Butler, S. Z., Hollen, S. M., Cao, L., Cui, Y., Gupta, J. A., Gutierrez, H. R., Heinz, T. F., Hong, S. S., Huang, J. and Ismach, A. F., et al. 2013. Progress, challenges, and opportunities in two- dimensional materials beyond graphene. *ACS Nano*. **4**: 2898–2926.

[2] Wang, Q. H., Kalantar-Zadeh, K., Kis, A., Coleman, J. N. & Strano, M. S. 2012. Electronics and optoelectronics of two-dimensional transition metal dichalcogenides. *Nature Nanotechnology*. **7**(11): 699–712.

[3] Bandaru, N. R. 2015. Structure and optical properties of transition metal dichalcogenides (TMDs)–MX2 (M= Mo, W & X= S, Se) under high pressure and high temperature conditions.
Doi: http://dx.doi.org/10.34917/7777293

[4] Greenwood, N. N. & Earnshaw, A. 2012. Chemistry of the elements. *Elsevier*.

[5] Eftekhari, A. 2017. Molybdenum di-Selenide (MoSe2) for energy storage, catalysis and optoelectronics. *Applied Materials Today*. *8*. **1**–17.
Doi: https://doi.org/10.1016/j.apmt.2017.01.006

[6] Shi, Y., Hua, C., Li, B., Fang, X., Yao, C., Zhang, Y., Hu, Y.-S., Wang, Z., Chen, L., Zhao. and Stucky, D.G. 2013. Highly ordered mesoporous crystalline MoSe2 material with efficient visible- light-driven photocatalytic activity and enhanced lithium storage performance. *Advanced Functional Materials.* **23**(14): 1832–1838.
Doi: https://doi.org/10.1002/adfm.201202144

[7] Kumar, A. & Ahluwalia, P. 2012. Electronic structure of transition metal dichalcogenides monolayers 1H-MX2 (M= Mo, W; X= S, Se, Te) from ab-initio theory: New direct band gap semiconductors. *The European Physical Journal B*. **85**: 1–7.

[8] Huang, H., Fan, X., Singh, D. J. & Zheng, W. 2020. Recent progress of TMD nanomaterials: Phase transitions and applications. *Nanoscale*. **12**(3): 1247–1268.

[9] Singh, E., Kim, K. S., Yeom, G. Y. & Nalwa, H. S. 2017. Atomically thin-layered molybdenum disulfide (mos2) for bulk-heterojunction solar cells. *ACS Applied Materials & Interfaces.* **9**(4): 3223–3245.
Doi: https://doi.org/10.1021/acsami.6b13582

[10] Roy, A., Movva, H. C., Satpati, B., Kim, K., Dey, R., Rai, A. & Banerjee, S. K. 2016. Structural and electrical properties of MoTe2 and MoSe2 grown by molecular beam epitaxy. *ACS applied materials & interfaces*. **8**(11): 7396-7402.
Doi: https://doi.org/10.1021/acsami.6b00961

[11] Ghosh,C., Sarkar, D., Mitra, M. & Chattopadhyay, K. 2013. Equi-biaxial strain: Tunable electronic structure and optical properties of bulk and monolayer mose2. *Journal of Physics d: Applied Physics*. **46**(39): 395304.
Doi: 10.1088/0022-3727/46/39/395304

[12] Kim, D. H. & Lim, D. 2017. The electrical and valley properties of monolayer MoSe2. *Current Applied Physics*. **17**(2): 321–325.
Doi: https://doi.org/10.1016/j.cap.2016.10.006

[13] Guan, X., Zhu, G., Wei, X. & Cao, J. 2019. Tuning the electronic properties of mono layer MoS2, MoSe2 and MoSSe by applying z-axial strain. *Chemical Physics Letters*. **730**: 191– 197.
Doi: https://doi.org/10.1016/j.cplett.2019.06.007

[14] Neupane, H. K. & Adhikari, N. P. 2021. Effect of vacancy defects in 2D vdW graphene/h- BN heterostructure: First-principles study. *AIP Advances*. **11**(8).
Doi: https://doi.org/10.1063/5.0059814

[15] Neupane, H. K. & Adhikari, N. P. 2021. Electronic and magnetic properties of defected MoS2 monolayer. *BIBECHANA*. **18**(2): 68-79.
Doi: http://nepjol.info/index.php/BIBECHANA

[16] Bartolotti, L. J. & Flurchick, K. 1996. *Reviews in Computational Chemistry*.Wiley.

[17] Giannozzi, P., Baroni, S., Bonini, N., Calandra, M., Car, R., Cavazzoni, C., Ceresoli, D., Chiarotti, G. L., Cococcioni, M. and Dabo, I. 2009. Quantum espresso: A modular and open-source software project for quantum simulations of materials. *Journal of physics: Condensed matter*. **21**(39): 395502.
Doi: 10.1088/0953-8984/21/39/395502

[18] Walker, B. & Gebauer, R. 2007. Ultrasoft pseudopotentials in time-dependent density- functional theory. *The Journal of Chemical Physics*. **127**(16).
Doi: https://doi.org/10.1063/1.2786999

[19] Perdew, J. P., Burke, K. & Ernzerhof, M. 1996. Generalized gradient approximation made simple. *Physical Review Letters*. **77**(18): 3865.
Doi: https://doi.org/10.1103/PhysRevLett.77.3865

[20] Vaught, A. 1996. Graphing with gnuplot and XMGR: Two graphing packages available under linux. *Linux Journal, 1996*(28es): 7–es.

[21] Kokalj, A. 1999. Xcrysden - a new program for displaying crystalline structures and electron densities. *Journal of Molecular Graphics and Modelling*. **17**(3-4): 176 179.
Doi: https://doi.org/10.1016/s1093-3263(99)00028-5

[22] Pack, J. D. and Monkhorst, H. J. 1977. Special points for Brillouin-zone integrations a reply. Phys. Rev. B. **16**(4): 1748.
Doi: https://doi.org/10.1103/physrevb.16.1748

[23] Togo, A. & Tanaka, I. 2015. First principles phonon calculations in materials science. *Scripta Materialia*. **108**: 1-5.
Doi: https://doi.org/10.1016/j.scriptamat.2015.07.021

[24] Ataca, C., Sahin, H. & Ciraci, S. 2012. Stable, single-layer mx2 transition-metal oxides and dichalcogenides in a honeycomb-like structure. *The Journal of Physical Chemistry C*. **116**(16): 8983–8999.
Doi: https://doi.org/10.1021/jp212558p

[25] Neupane, H. K. & Adhikari, N. P. 2021. Structural, electronic and magnetic properties of defected water adsorbed single-layer MoS2. *Journal of Institute of Science and Technology*. **26**(1): 43-50.

[26] Knop, O. & MacDonald, R. D. 1961. Chalkogenides of the transition elements III: molybdenum ditelluride. *Canadian Journal of Chemistry*. **39**(4): 897-904.
Doi: https://doi.org/10.1139/v61-110

[27] Puotinen, D. & Newnham, R. 1961. The crystal structure of molybdenum ditelluride. *Acta Crystallographica.* **14**: 691-692.
Doi: https://doi.org/10.1107/S0365110X61002084

[28] Neupane, H. K., Oli, D., Rijal, O. S., Neupane, R. K., Shrestha, P., Sharma, S. & Parajuli**,** R. 2025. Exploring the structural, dynamical, mechanical, electronic, magnetic and optical properties of Ta2AlN, Ti2AlN & Ti2GaN MAX phase compounds:
First principles study. *Heliyon*. **11**(6)
Doi: https://doi.org/10.1016/j.heliyon.2025.e42962

[29] Rijal, O. S., Neupane, H. K., Oli, D., Neupane, R. K., Shrestha, P., Sharma, S. & Parajuli, R. 2025. A first-principles investigation of the structural, mechanical, dynamic, electronic, magnetic, and optical properties of Ti2AC (A= Cd, S) MAX phase compounds. *Journal of Physics D: Applied Physics*. **58**(12): 125102.
Doi: 10.1088/1361-6463/ada808

[30] Ma, Y., Dai, Y., Guo, M., Niu, C., Lu, J. & Huang, B. 2011. Electronic and magnetic properties of perfect, vacancy-doped, and nonmetal adsorbed MoSe2, MoTe2 and WS2 monolayers. *Physical Chemistry Chemical Physics.* **13**(34): 15546–15553.
Doi: https://doi.org/10.1039/C1CP21159E

[31] Tongay, S., Zhou, J., Ataca, C., Lo, K., Matthews, T. S., Li, J., Grossman, J. C. & Wu, J. 2012. Thermally driven crossover from indirect toward direct bandgap in 2d semiconductors: Mose2 versus mos2. *Nano Letters.* **12**(11): 5576–5580.

[32] Neupane, H. K. & Adhikari, N. P. 2020. Tuning structural, electronic, and magnetic properties of C sites vacancy defects in Graphene/MoS2 van der Waals heterostructure materials: A first-principles study. *Advances in Condensed Matter Physics.* **2020**(1): 8850701.
Doi: https://doi.org/10.1155/2020/8850701

[33] Neupane, H. K. & Adhikari, N. P. 2022. Adsorption of water on C sites vacancy defected graphene/h-BN: first-principles study. *Journal of Molecular Modeling*. **28**(4): 107**.**